Polarization-driven single qubit Pauli gates using Si_3N_4 race-track ring resonator

SAPNA TIWARI[1], GAURAV KUMAR BHARTI[2,*], AHMAD S. ABDULLAH[3]

[1]Advanced Photonics and Cyber Physical system Lab, Department of Electronics and Communication Engineering, Indian Institute of Information Technology Bhopal, India
[2]Department of Electrical, Electronics and Communication Engineering, Galgotias University, Greater Noida, 203201, India
[3]Department of Communication Engineering, College of Engineering, University of Diyala, Baghdad st., Baqubah, 32001 Diyala, Iraq

Quantum logic gates play a significant role as the fundamental building block for both quantum computing and quantum communication processes. The proposed paper highlights the implementation of different Pauli's quantum gate using silicon nitride-based racetrack configured ring resonator. The polarization rotation is noted at the $\lambda \sim 1529.5$ nm. The different Pauli's gate is perceived at the resonance wavelength of 1529.5 nm, by changing the azimuth as well as elliptical angle of the input light. The proposed model is fast and efficient. The proposed polarization driven Pauli's quantum gate has been validated using the jones matrix and numerical simulation.

1. Introduction

Quantum technology exhibits the ability to deal with a vast amount of information concurrently, which distinguishes it from classical information processing [1, 2]. The usage of qubits is the significant component for quantum computing applications. The fundamental component essential for quantum computing is the quantum gate, which can be classified into three distinct categories: single qubit gates, two qubit gates, and multiqubit gates [1]. The proposed paper revolves around the concept of polarization rotation in a race-track ring-resonator, which is characterized by changes in both the azimuth (ψ) and elliptical angle (χ). In this work, the results from numerical simulation for polarization rotation has been validated using the jones matrix [1, 2, 3].

Compared to its electronic counterpart, photonics offers superior speed and bandwidth [2, 4, 5]. The limitations of conventional electronic circuits have been addressed through the development of photonic circuits [2, 6]. While electronic devices struggle with data processing delays, photonics minimizes this issue by utilizing photons as information carriers. The rapid propagation speed of photons, comparable to light, and their ease of manipulation make optical devices more advantageous [1,5,7]. Researchers have reported various optical components for computing applications [1, 3]. Among these, the MZI and Race Track Ring Resonator (RTRR) are prominent, RTRR overcomes many of the shortcomings existing in other optical structures [7-9]. It offers significant advantages, including lower operating power, simpler design, ease in fabrication processes,

compact size, high bandwidth and speed [8, 9]. RTRR have various applications, including optical filtering, wavelength division multiplexing, optical sensing, optical switching, and quantum computing [7, 8, 9, 10, 11]. The literature has documented the development of integrated Pauli X, Y, and Z gates based on photonic crystals, employing intensity and phase encoding techniques [2, 6, 9, 12]. To achieve the implementation of single-qubit gates, researchers have utilized $LiNbO_3$-based electro-optic material for modifying intensity and phase characteristics [12]. Fig. 1 depicts the fundamental optical Circular Ring Resonator (RR) structure, which consists of a circular ring configuration positioned above straight waveguide. As shown in Fig. 1, the RR features two ports: one for injecting the input signal and another for observing the output. Optimal coupling of the incoming signal to the ring structure occurs under resonance conditions. This phenomenon arises due to constructive interference when a light signal traverses an optical path equal to a whole-number multiple of the wavelength, resulting in maximum light intensity at the output ports [13-17]. The scenario in which maximum output is achieved at the output port is referred to as the resonant condition or ON state. Conversely, the RR is considered to be in the OFF state when the input light signal from the bus waveguide does not couple with the ring structure. This condition occurs only when there is a change in the refractive index (RI) of the ring material, an alteration in the ring's dimensions, or other geometrical factors [17-20].

In this paper, RTRR has been utilized to implement the Pauli single qubit X, Y, and Z gates by modifying the azimuth and elliptical angle of the input polarized light.

The RTRR is employed to perform all-optical switching operations in the all-optical system [2]. RTRR, an optical device, demonstrates exceptional all-optical switching capabilities [13, 14]. The polarization rotation has been achieved by enhancing geometry induced birefringence of the device and with the insertion of the polarization-rotator (PR) in the race-track-shaped RR as shown in Fig. 2 [2]. The geometry-induced birefringence of the device has been enhanced by optimizing the height and width of the RTRR waveguide. The PR in the proposed device rotates the polarization axis of an input polarized light by an angle of 30 deg. The tightly curved bending waveguide of the race-track architecture of the RR also supports the polarization rotation phenomena. The structure of the ring resonator is composed of Si_3N_4 material. The properties of low loss and ease of fabrication render Si_3N_4 an ideal resource for RTRR design [1, 3, 4, 5].

Fig. 1. RR structure (colour online)

2. Pauli gates

Pauli gates are vital for single qubit operations that are fundamental in operating quantum states. Comprising three gates represented by the Pauli matrices *X*, *Y*, and *Z*, these processes serve as vital components in constructing more intricate quantum circuits and algorithms. The Pauli gates enable state manipulation and form the basis for implementing larger quantum operations [2-4]. The Pauli gates are defined as: *Pauli-X gate (X-gate)*: Its working is similar to the classical NOT gate, which inverts the qubit state from |0> to |1> and vice versa. It rotates the qubit state around the Bloch sphere's *X-axis* by *π radians*.

Pauli-Y gate (Y-gate): The working of this gate combines the effects of *Pauli-X gate* and *Pauli-Z gate*, performing a bit flip as well as a phase flip on the qubit. It rotates the qubit state around the Bloch sphere's *Y-axis* by *π/2 radians*.

Pauli-Z gate (Z-gate): It applies a phase flip to the qubit state, preserving the basis states |0> and |1> while reversing the relative phase of |1>. It rotates the qubit state from one place to another the Bloch sphere's *Z-axis* by *π radians*.

In quantum computing, a bit-flip and a phase-flip refer to different types of transformations applied to qubit states. A flip, also known as a bit-flip, is a transformation that changes the state of a qubit from |0> to |1> or from |1> to |0>, just like a classical NOT gate changes the state of a classical bit from 0 to 1 or 1 to 0. The *X-gate* performs this flip operation on qubits. When applied to a qubit, the *X-gate* essentially swaps the amplitudes of the |0> and |1>

states. A phase-flip is a transformation that changes the relative phase of the |1> state without changing the |0> state. In the phase-flip, only the change in qubit state has been observed. The change in actual basis state has not been observed. The *Z-gate* is responsible for phase flips. When applied to a qubit, the *Z-gate* changes the sign of the amplitude of the |1> state, while the amplitude of the |0> state remains the same.

3. Modelling of the device

The all-optical polarization rotation is performed using a RTRR to create an all-optical quantum gate. RTRR is an optical device that possesses remarkable all-optical polarization capabilities [7]. In this model, the polarization rotation has been noticed due to establishing relationship between the azimuth angle (ψ) and the elliptical angle (χ). The height, width, and the other geometrical parameters of the RTRR waveguide are optimized to enhance the geometry-induced birefringence, as it affects the polarization and propagation of light. The proposed architecture includes a PR to facilitate the polarization rotation/conversion phenomena. Additionally, the tightly curved bending waveguide of the race track architecture in the RTRR supports the polarization rotation phenomenon [8, 9, 13, 15, 17]. In this paper, polarization rotation in RTRR is observed at the output and its response changes as a function of the pump nature (or incident pump history) and thus can be used to design quantum gates. Fig. 1 shows the proposed device model and the waveguide cross-section in inset. The polarization rotation in RTRR is described in terms of the change in the azimuth angle (ψ), elliptical angle (χ) as well as by employing a segment of PR that rotates the polarization axis of an input light. We have considered the cut-off angle of 45° for Pauli -X gate. The angle below this angle this is |0> otherwise it is |1>. Further, an angle 5° has been considered as a tolerance angle margin for both ψ and χ.
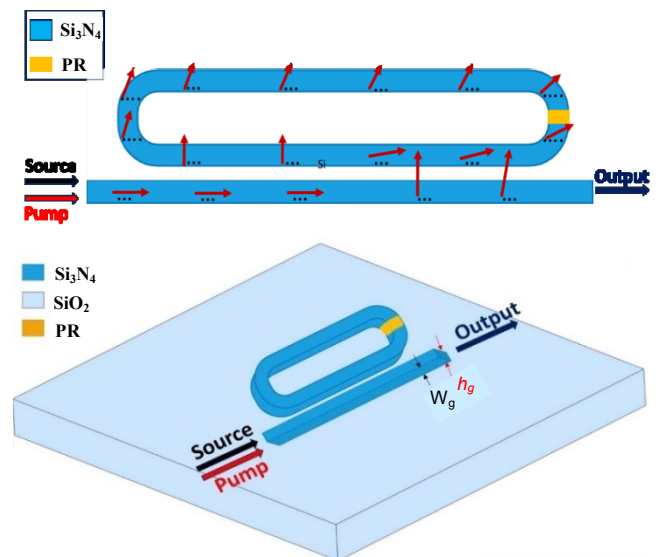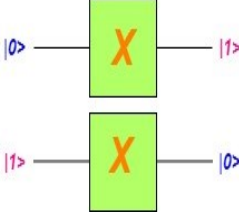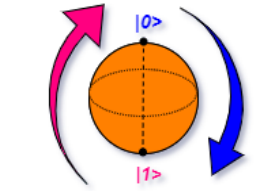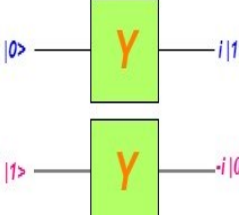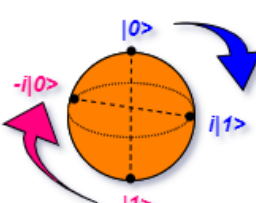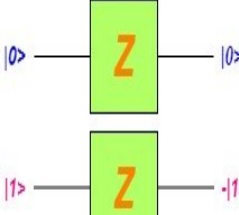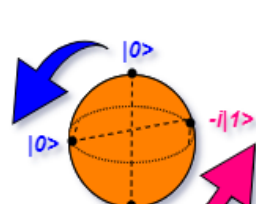

Fig. 2. Proposed structure (colour online)

The quantum gate operation can be represented by the transformation on the Bloch Sphere [1, 21]. When a gate operates on input qubit, output state has been changed. In the Bloch sphere representation, the qubit rotating the point representing the qubit's state around a specific axis, as shown in Table 1. The foundation of quantum computation principles is rooted in Pauli matrices, as described in the literatures [20-32]. Within the quantum gate family *Pauli gates* function as single-qubit gates. This innovative approach demonstrated satisfactory performance, thereby validating its potential as a fundamental building block for future photonics integrated circuit (PIC) implementations that possess significant characteristics [23, 24, 25]. The successful integration of RTRR-based polarization control with quantum gate functionality covers the way for the development of scalable, efficient, and robust quantum computing architectures and future wearable and IoT devices [33]. Table 1 illustrates the representation of these gates along with their corresponding Bloch sphere visualizations.

Table 1. Symbol and Bloch sphere representation of Pauli's Gates (colour online)

Symbol	Bloch Sphere

The RTRR architecture is utilized in the model to attain polarization rotation, as it has the capability to alter the polarization state while propagating in the waveguide [7, 17]. Polarized light possesses a fixed phase for its field components, which vary from one another. The two orthogonal components are used to define a state of polarization. When propagating a light beam, the complex amplitudes E_x and E_y are typically denoted as below [7].

$$E_x = A_x e^{i\partial x} \qquad \text{i (a)}$$
$$E_y = A_y e^{i\partial y} \qquad \text{i (b)}$$

The polarization of a beam can be characterized using the magnitudes (A_x, A_y) and phase angles ($\partial x, \partial y$ of its x and y components of the electric field component). These complex amplitudes, as expressed in Eq. (i), containing all the information about the polarization state of the wave. In the jones vector, the polarized light can be written as Eq. i (a) and i (b) [7,8].

$$E = \begin{bmatrix} Ex \\ Ey \end{bmatrix} = \begin{bmatrix} Ax e^{i\partial x} \\ Ay e^{i\partial y} \end{bmatrix} \qquad \text{(ii)}$$

The Jones matrix, a mathematical framework for describing polarized light, is parameterized by the amplitudes and the polarization angle ψ, as extensively documented in literature [7,8]. This matrix provides a comprehensive representation of the polarization state, enabling precise analysis and modeling of optical phenomena.

$$E = \begin{bmatrix} Ex \\ Ey \end{bmatrix} = \begin{bmatrix} Ax \cos \psi \\ Ay \sin\psi \end{bmatrix} \qquad \text{(iii)}$$

In the proposed design, the qubit states of |0> and |1> are represented by the azimuth angle (ψ) of 0^0 and 90^0 and the phase change in *Pauli gates* are represented by elliptical angle (χ) respectively. Based on the simulation results, it can be inferred that the proposed model can function as a quantum gate that converts the (|0>) state to the (|1>) and vice versa as shown in the form of matrix below.

$$|0> = \begin{bmatrix} Ax \cos \psi \\ 0 \end{bmatrix} = \begin{bmatrix} 1 \\ 0 \end{bmatrix} \qquad \text{(iv)}$$

When azimuth angle $\psi = 90^0$. The generalized Jones matrix for *Pauli gate* can be written as below.

$$|1> = \begin{bmatrix} 0 \\ Ay \sin\psi \end{bmatrix} = \begin{bmatrix} 0 \\ 1 \end{bmatrix} \qquad \text{(v)}$$

The model highlights the implementation and verification of Pauli gates utilizing Jones vectors in photonics-based quantum computing.

4. Working

RTRR works on the principle of evanescent coupling, where light is introduced into the optical circuit through the input port. and travels through the straight waveguide after the round-trip [15, 16, 18]. When the wavelength of the input light matches the resonance wavelength of the race track resonator, the light is transferred from the straight waveguide to the race-track resonator. The light therefore, circulates within the resonator, creating a standing wave pattern, and is coupled race-track, comes out from output port [21, 22]. By simulating and optimizing the design

parameters of the device, the all-optical quantum gates has been realized in the paper. The suggested design features a single waveguide RTRR with a PR constructed from birefringent material [5,7,8]. PR is integrated into the RTRR's race track waveguide arm, using CMOS technology [8]. Angular transmission through the PR results in alterations to the ψ and χ [7]. To achieve polarization rotation in the RTRR, the PR's rotation angle is set at 30 degrees, while pump characteristics are adjusted to modify the azimuth and elliptical angle. The circuit is simulated using a photonics integrated simulator [9]. The schematic of the design structure for simulation is illustrated in Fig. 3. In this proposed configuration, a 1529.5 nm wavelength input pulse is introduced to the device, and the resulting changes are observed in ψ and χ. The configuration shown in Fig. 3 is equivalent to model shown in Fig. 2. The key morphological characteristics used for simulation are shown in Table 2.

Table 2. Geometrical parameters used in the simulation

Parameters	Description
Substrate material	*Si*
Waveguide material	Si_3N_4
Coupling coefficient	0.5,0.15
Input Power	1.85 *mW*
Circumference of the RTRR	63 *μm*
Coupling length	3 *μm*
RI of RTRR	3.47
Input Wavelength	1529.5 *nm*
Simulation Method	FDTD
Polarizer Angle	30^0
Input Light Nature	Gaussian Pulse
Central Wavelength	1529.5 nm

(a)   Simple to Compound View of Model
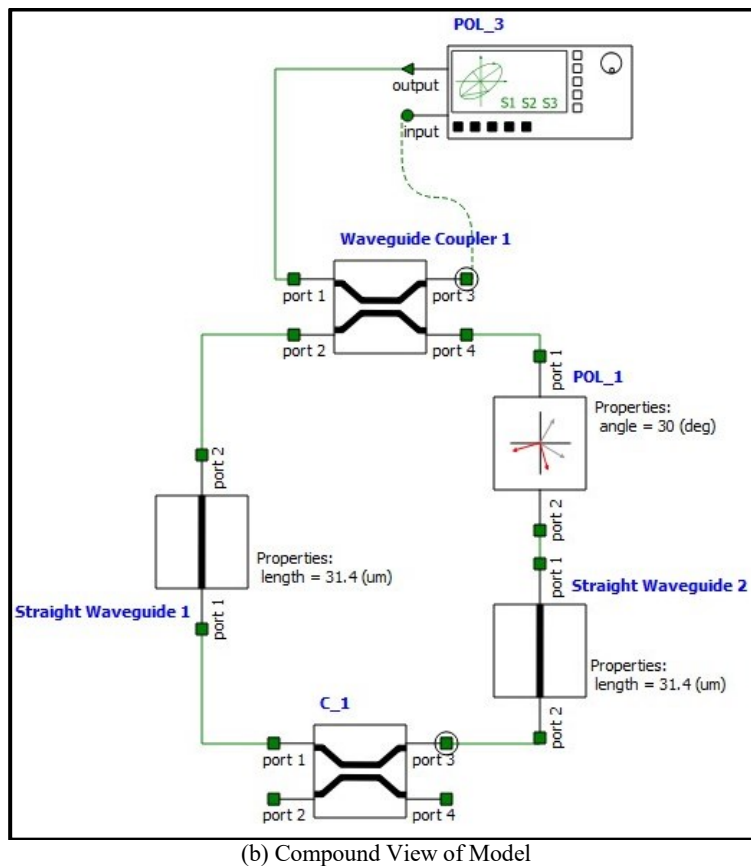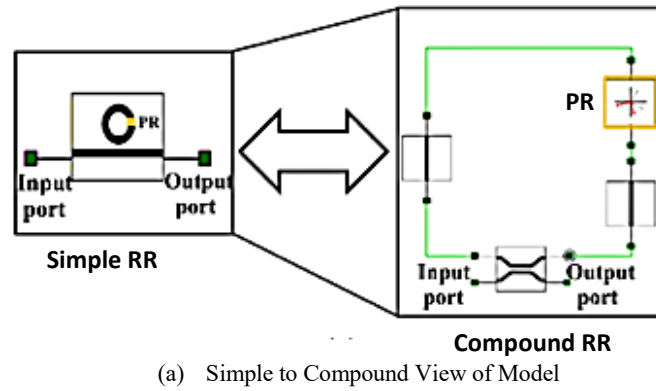

(b) Compound View of Model

Fig. 3. Schematic of the model (colour online)

The input-output relationship of the proposed design is highlighted in Table 3.

Table 3. Input-Output relationship of Pauli Gates

Quantum gate	Input qubit	Output qubit	Phase condition
X Gate	$\lvert 0\rangle = \begin{pmatrix} 1 \\ 0 \end{pmatrix}$	$\lvert 1\rangle = \begin{pmatrix} 0 \\ 1 \end{pmatrix}$	Same phase
	$\lvert 1\rangle = \begin{pmatrix} 0 \\ 1 \end{pmatrix}$	$\lvert 0\rangle = \begin{pmatrix} 1 \\ 0 \end{pmatrix}$	Same phase
Y Gate	$\lvert 0\rangle = \begin{pmatrix} 1 \\ 0 \end{pmatrix}$	$i\lvert 1\rangle = \begin{pmatrix} 0 \\ i \end{pmatrix}$	Phase lead by $\pi/2$
	$\lvert 1\rangle = \begin{pmatrix} 0 \\ 1 \end{pmatrix}$	$-i\lvert 0\rangle = \begin{pmatrix} -i \\ 0 \end{pmatrix}$	Phase lag by $\pi/2$
Z Gate	$\lvert 0\rangle = \begin{pmatrix} 1 \\ 0 \end{pmatrix}$	$\lvert 0\rangle = \begin{pmatrix} 1 \\ 0 \end{pmatrix}$	Same phase
	$\lvert 1\rangle = \begin{pmatrix} 0 \\ 1 \end{pmatrix}$	$-\lvert 1\rangle = \begin{pmatrix} 0 \\ 1 \end{pmatrix}$	Phase lag by π

5. Results

The proposed work highlights the optical polarization in RTRR for quantum gate designing, specifically implementing the Pauli gate through numerical modeling of the structure. The state of the polarization of the ψ and χ resembles the working of quantum *Pauli gates*.

Case I. Pauli X Gate

When the signal incident at an azimuth angle (ψ) and elliptical angle (χ) of 0^0 resembling $\lvert 0\rangle$, the output port displays ψ of 87.88^0 and χ of 0^0 resembling $\lvert 1\rangle$, as depicted in Fig. 4 (a) and Fig. 4 (b). If the input pump with ψ of 90^0 and χ of 0^0 resembling $\lvert 1\rangle$ is applied to the input port of RTRR, the monitor observes ψ of 1.23^0 and χ of 0^0 resembling $\lvert 0\rangle$, as shown in Fig. 4 (c) and Fig. 4 (d). The work presented employed the concept of polarization in RTRR for designing the *Pauli-X gate* operation as discussed in the previous section of this paper. Numerical modelling of the RTRR has been conducted to implement the *Pauli-X gate*. The azimuth and elliptical angles of the output light signal is used to design the quantum *Pauli-X gate*.

Table 4. Single qubit Pauli X gate

Input			Output		
Qubit	ψ	χ	ψ	χ	Qubit
$\lvert 0\rangle$	0^0	0^0	87.88^0	0^0	$\lvert 1\rangle$
$\lvert 1\rangle$	90°	0^0	1.23^0	0^0	$\lvert 0\rangle$

Case II. Pauli Y Gate

When the signal incident at an ψ of 0^0 and χ of 45^0, resembling phase change of $\pi/2$ is applied to the input port of RTRR, the output port displays an ψ of 87.88^0 and χ with a leading phase change, as depicted in Fig. 5(a) and Fig. 5(b). If the input pump with ψ of 90^0 and χ of -45 resembling phase change of $-\pi/2$ is applied to the input port of RTRR, then the monitor observes an ψ of 1.23^0 and χ with a leading phase change observed as shown in Fig. 5(c) and Fig. 5(d). The work presented employed the concept of polarization in RTRR for designing the *Pauli-Y gate* operation. Numerical modeling of the RTRR has been conducted to implement the *Pauli-Y gate*.

Table 5. Operation of proposed single qubit Pauli Y gate

Input			Output		
Qubit	Ψ	χ	ψ	χ	Qubit
$\lvert 0\rangle$	0^0	45^0	87.88	29.9^0 (lead)	$i\lvert 1\rangle$
$\lvert 1\rangle$	90°	-45^0	1.23^0	-23.5^0 (lag)	$-i\lvert 0\rangle$

Case III. Pauli Z Gate

The output port of the RTRR without a PR exhibits a ψ of 0^0 and χ with no phase change is observed. The results are demonstrated in Fig. 6 (a)-(d) and highlighted in Table 6.

The change of π phase in pauli-Z gate can be resembled by the negative sign of the matrix. The value mentioned in Table 6 indicates the π phase shift in the pauli Z-gate. Thus, the values mentioned in Table 6 validates pauli Z-gates.

The Pauli-Z gate is defined as a single-qubit quantum operator that applies a π-phase shift to the |1⟩ computational basis state while leaving the |0⟩ state unchanged. Mathematically, it is represented as:

Z=[100 −1], which corresponds to a rotation of the qubit state by π around the Z-axis of the Bloch sphere.

In Table 6 of the paper, the simulation results clearly validate this behavior. The table lists the input and output azimuth (ψ) and elliptical (χ) angles for the Pauli-Z gate. Specifically:

- For |0⟩, the output polarization state (ψ, χ) remains unchanged — implying no relative phase shift.
- For |1⟩, the output polarization exhibits a measurable elliptical angle shift of −24.40°, corresponding to a π-phase inversion of the |1⟩ state.

This observed change in elliptical angle (χ) signifies a phase shift introduced exclusively to the |1⟩ component, without amplitude change in the |0⟩ component, which is exactly the characteristic action of the Pauli-Z gate. Hence, the results in Table 6 justify that the device correctly implements the Pauli-Z gate by imparting a π phase on the |1⟩ state.

Table 6. Operation of proposed single qubit Pauli Z gate

Input			Output		
Qubit	ψ	χ	ψ		Qubit
|0>	0^0	0^0	0^0	0^0	|0>
|1>	90^0	-45	73^0	-24.4^0	-|1>

Fig. 4. (b) Elliptical angle of 0^0 (colour online)
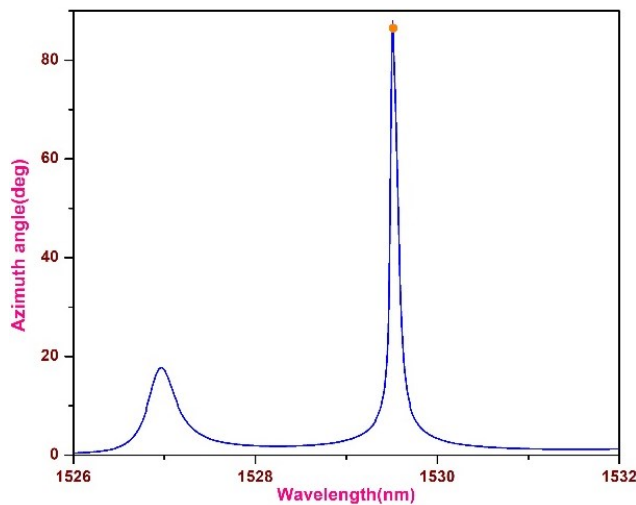
Fig. 4. (c) Azimuth angle of 1.23^0 (colour online)

Fig. 4. (a) Azimuth angle of 87.88^0 (colour online)

Fig. 4. (d) Elliptical angle of 0^0 (colour online)

Fig. 5. (a) Azimuth angle of 87.88^0 (colour online)

Fig. 5. (d) Elliptical angle of Phase lag (colour online)

Fig. 5. (b) Elliptical angle of Phase lead (colour online)

Fig. 6. (a) Azimuth angle of 0^0 (colour online)

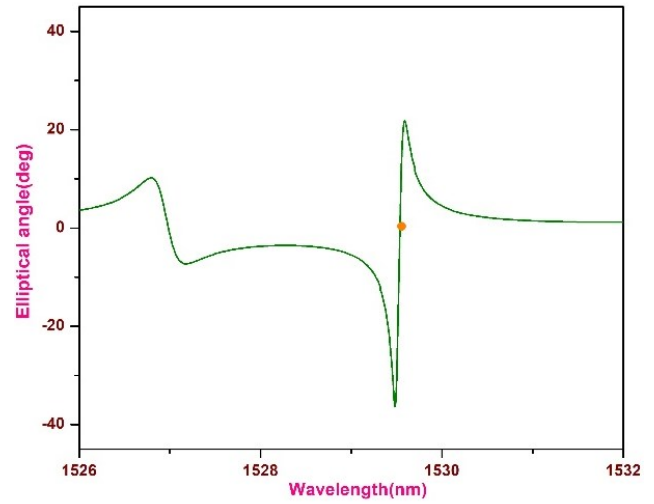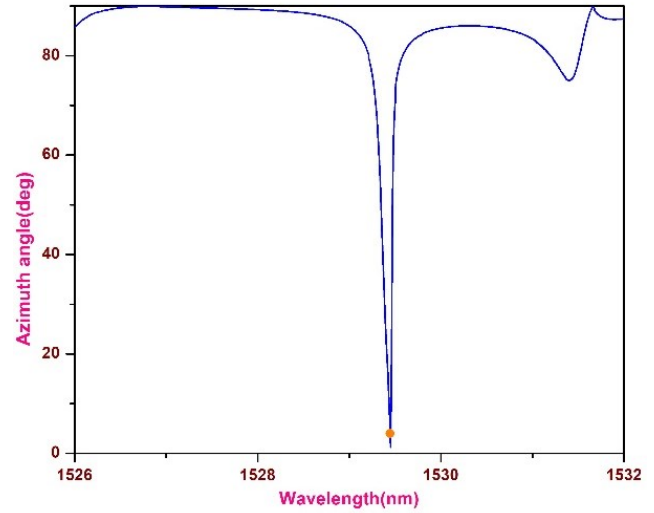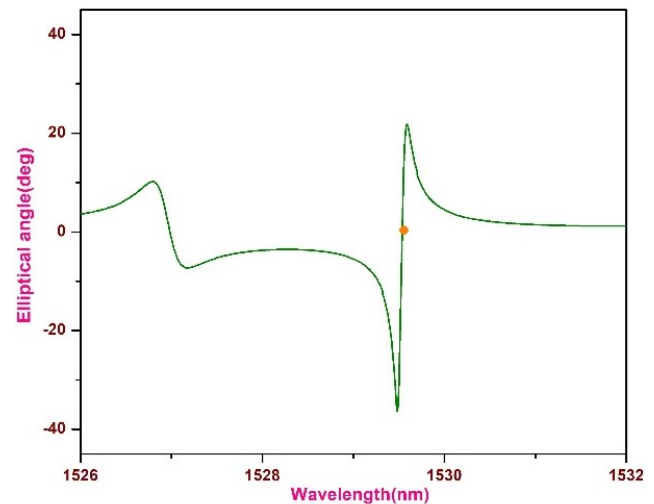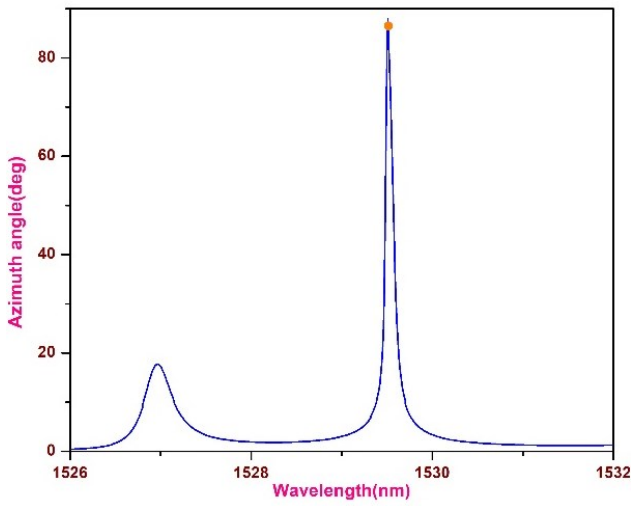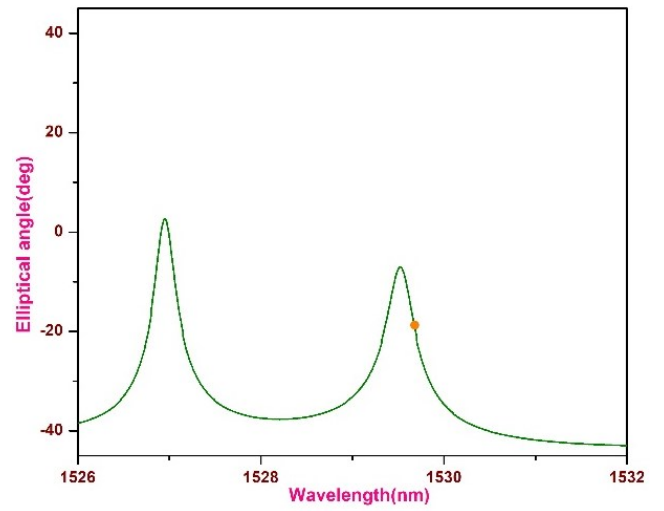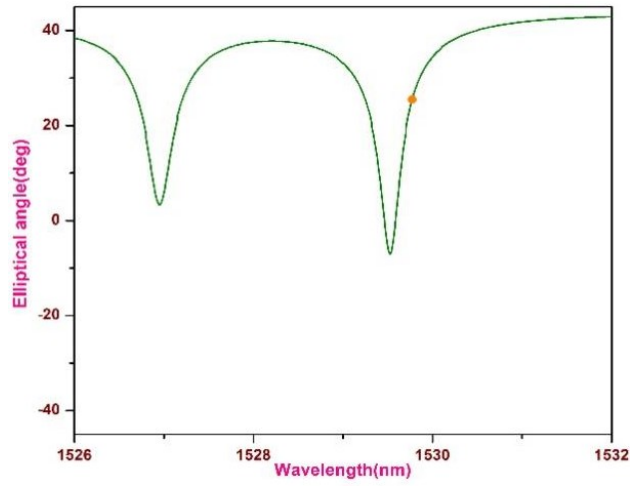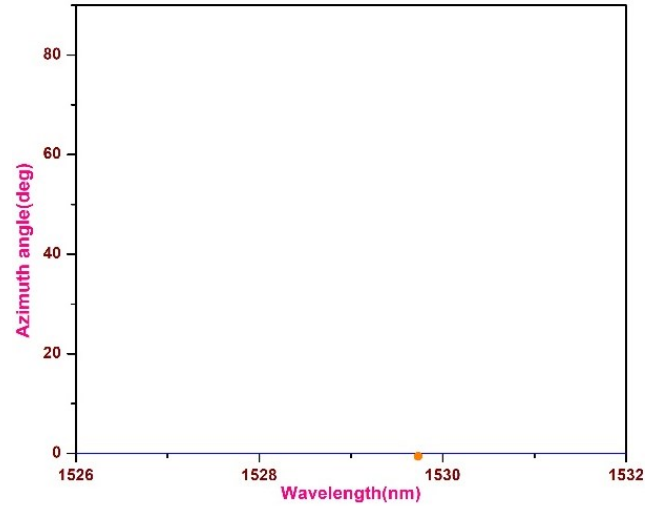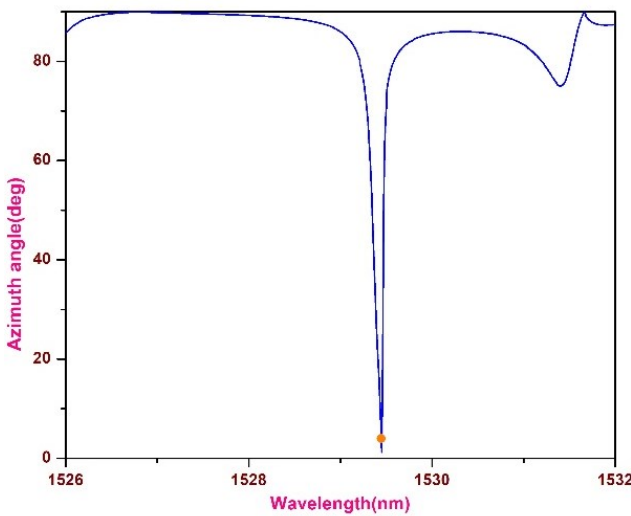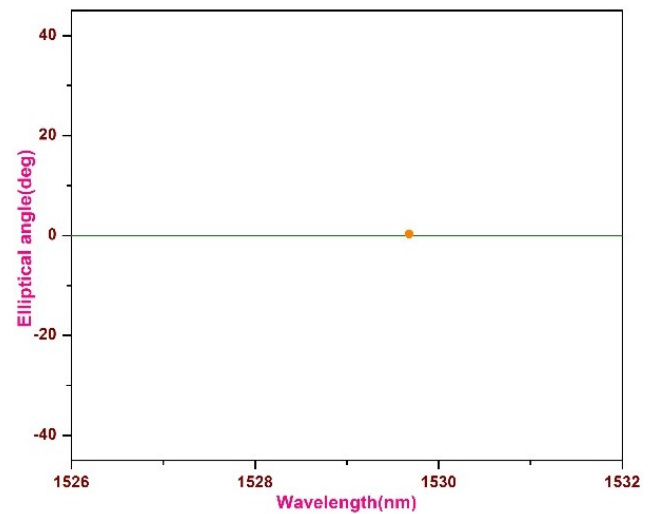*Fig. 5. (c) Azimuth angle of 1.23^0 (colour online)*

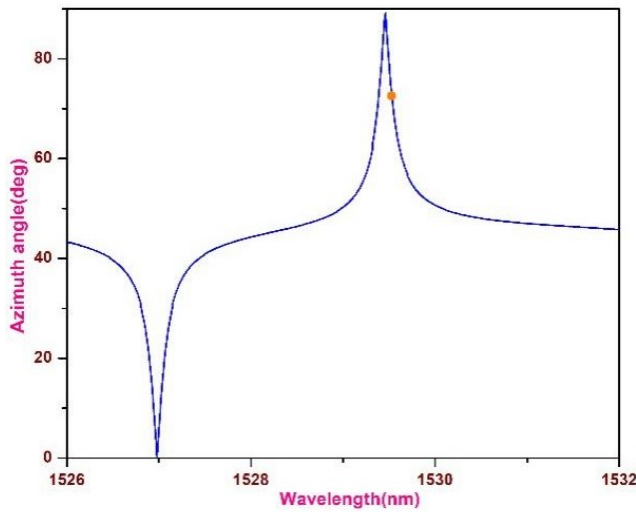*Fig. 6. (b) Elliptical angle of 0^0 (colour online)*

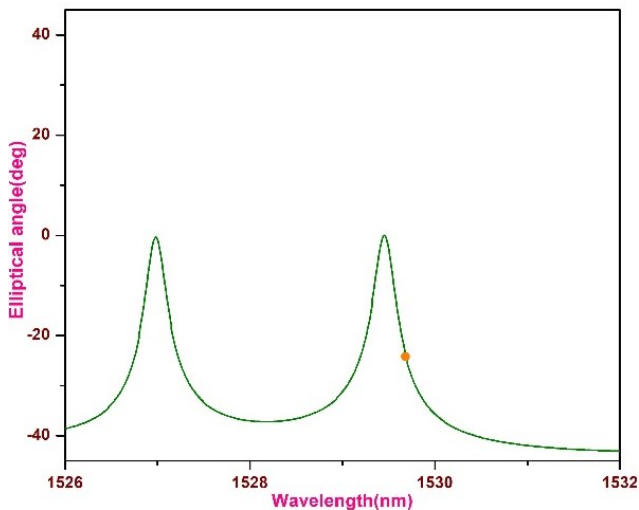*Fig. 6. (c) Azimuth angle of 73⁰ (colour online)*

Fig. 6. (d) Elliptical angle of 0⁰ (colour online)

6. Discussion

The proposed simulation is conducted using the commercial-grade INTERCONNECT simulation platform and the simulation study utilized a fixed polarized input

source with a central wavelength of 1529.5 nm. To optimize polarization conversion, the circumference of the structure is set to 63 *μm* after doing optimization and sweep. Symmetric coupling coefficients of 0.5 has been chosen, validated through a vast literature survey. The gap between the straight waveguide and the ring waveguide is 0.001 nm.

The pump power of 1.85 *mW* with gaussian source is applied. The input pump power is same in all the cases. To analyze polarization rotation, both azimuth and elliptical angles are varied, allowing for a comprehensive understanding of the RTRR polarization conversion capabilities. The extinction parameter is important in designing Pauli Gates as it signifies the difference between the higher value and the lower value. The maximum value of extinction ratio (ER) is desirable. The ER value of 19.39 dB is noted from the simulation. Response time is defined as the time to observe output at the output port after injecting input from the input port of the device. Switching time is defined as the time to change the output from one state to another.

The response time is calculated by placing the monitor during simulation to determine the response.

The presented work demonstrated a satisfactory performance, validating its potential as a fundamental unit for future challenging photonics integrated circuit implementation by estimating the optimum performance parameters. The few performance parameters are mentioned in Table 7. Additionally, the presented single qubit Pauli's gates show significant performance in terms of its compactness, and propagation losses. Here, the overall losses including the propagation loss, material loss and the dispersion loss. The losses it determined by the using the "Interconnect" and the "FDTD" simulation.

The design is compatible with CMOS fabrication technology. To understand the significance of the presented work, the comparison with the recent literatures is presented in Table 8.

Table 7. Performance parameters

Parameter	Value
Extinction ratio	19.39 dB
Overall losses of the device	6.03db/cm
Response Time	0.5 ps
Finesse	8.3 nm

Table 8. Comparison with the recent literatures

Ref. No.	Platform	ER	Response time	Losses	Technology
[2]	*PhC*	-	0.36 ps	-	Wavelength Encoding
[6]	*Si*	19.39	-	Insertion loss - −0.13 dB	Intensity and input light phase variation
[9]	*EO Modulator*	-	-	-	Pockels' Effect
[12]	*EO Modulator*	-	-	-	Phase Encoding
Present Work	*Si₃N₄*	19.39 dB	0.5 ps	6.03dB/cm	Polarization and input light phase variation

7. Conclusion

The proposed work leverages the concept of optical polarization in RTRR to facilitate quantum gate operations, specifically implementing *the Pauli X, Y and Z gate* through numerical modeling. Notably, the polarization state, defined by the azimuth angle (ψ) and elliptical angle (χ), exhibits a outstanding resemblance to the operational principles of quantum *Pauli X, Y and Z gates*.

References

[1] K. K. Choure, A. Saharia, N. Mudgal, R. Pandey, M. Prajapat, R. K. Maddila, M. Tiwari, G. Singh, Optics & Laser Technology **170**, 110263 (2024).

[2] Sarfaraj, Mir Nadim, Sourangshu Mukhopadhyay, Optics Communications **550**, 129913 (2024).

[3] K. K. Choure, G. K. Bharti, A. Saharia, N. Mudgal, A. Bhatnagar, G. Singh, Optical and Quantum Electronics **54**(5), 276 (2022).

[4] K. K. Choure, G. K. Bharti, A. Saharia, N. Mudgal, G. Singh, International Conference on Optical and Wireless Technologies pp. 375-380 (2021).

[5] G. K. Bharti, R. K. Sonkar, Optical Engineering **60**(8), 085109 (2021).

[6] P. De, S. Ranwa, S. Mukhopadhyay, Optics & Laser Technology **152**, 108141 (2022).

[7] M. P. Singh, M. Hossain, J. K. Rakshit, G. K. Bharti, J. N. Roy, Brazilian Journal of Physics **51**(6), 1763 (2021).

[8] M. P. Singh, J. K. Rakshit, M. Hossain, S. Mandal, J. N. Roy, Journal of Optics **53**(3), (2024).

[9] B. Sarkar, S. Mukhopadhyay, J. Opt. **46**, 143 (2017).

[10] M. P. Singh, J. K. Rakshit, M. Hossain, J. N. Roy, Optical and Quantum Electronics **54**(5), 287 (2022).

[11] G. K. Bharti, M. P. Singh, J. K. Rakshit, Silicon **12**, 1279 (2020).

[12] M. N. Sarfaraj, S. Mukhopadhyay, Optoelectron. Lett. **17**, 746 (2021).

[13] S. Dey, S. Mukhopadhyay, J. Opt. **48**, 520 (2019).

[14] C. Manolatou, M. J. Khan, S. Fan, P. R. Villeneuve, H. A. Haus, J. D. Joannopoulos, IEEE Journal of Quantum Electronics **35**(9), 1322 (1999).

[15] J. E. Heebner, Vincent Wong, A. Schweinsberg, R. W. Boyd, D. J. Jackson, IEEE Journal of Quantum Electronics **40**(6), 726 (2004).

[16] Chris G. H. Roeloffzen, Marcel Hoekman, Edwin J. Klein, Lennart S. Wevers, Roelof Bernardus Timens, Denys Marchenko, Dimitri Geskus, Ronald Dekker, Andrea Alippi, Robert Grootjans, Albert van Rees, Ruud M Oldenbeuving, Jörn P Epping, René G Heideman, Kerstin Wörhoff, Arne Leinse, Douwe Geuzebroek, Erik Schreuder, Paulus WL van Dijk, Ilka Visscher, Caterina Taddei, Youwen Fan, Caterina Taballione, Yang Liu, David Marpaung, Leimeng Zhuang, Meryem Benelajla, Klaus-J Boller, IEEE Journal of Selected Topics in Quantum Electronics **24**(4), 1 (2018).

[17] Wolfgang Freude, Alexander Kotz, Hend Kholeif, Adrian Schwarzenberger, Artem Kuzmin, Carsten Eschenbaum, Adrian Mertens, Sidra Sarwar, Peter Erk, Stefan Bräse, Christian Koos, IEEE Journal of Selected Topics in Quantum Electronics **30**(4), 1 (2024).

[18] R. Soref, IEEE Journal of Selected Topics in Quantum Electronics **12**(6), 1678 (2006).

[19] Y. Gu, Yuchen, Weng, Yishi, Wei, Ran, Shen, Zhongwen, Wang, Chuang, Zhang, Li Xuan, Zhang Yuning, IEEE Photonics Journal **14**(1), 1 (2022).

[20] G. Brunetti, R. Heuvink, E. Schreuder, M. N. Armenise, C. Ciminelli, IEEE Photonics Technology Letters **35**(22), 1215 (2023).

[21] G. K. Bharti, J. K. Rakshit, Photon. Netw. Commun. **35**, 381 (2018).

[22] M. Hossain, M. P. Singh, J. K. Rakshit, Silicon **14**, 5601 (2022).

[23] P. Gupta, A. Agrawal, N. K. Jha, IEEE Transactions on Computer-Aided Design of Integrated Circuits and Systems **25**(11), 2317 (2006).

[24] B. Tan, J. Cong, IEEE Transactions on Computers **70**(9), 1363 (2021).

[25] C. Hughes, J. Isaacson, A. Perry, R. F. Sun, J. Turner, Quantum Gates, Quantum Computing for the Quantum Curious, Springer, Cham, 2021.

[26] M. Hassangholizadeh-Kashtiban, H. Alipour-Banaei, M. B. Tavakoli, Reza Sabbaghi-Nadooshan J. Comput. Electron. **19**, 1281 (2020).

[27] R. Talebzadeh, R. Beiranvand, S. H. Moayed, Opt. Quant. Electron. **55**, 241 (2023).

[28] M. N. Sarfaraj, S. Mukhopadhyay, Optics Communications **579**, 131520 (2025).

[29] Savarimuthu Robinson, Rangaswamy Nakkeeran, Optical Engineering **52**(6), 060901 (2013).

[30] M. N. Sarfaraj, S. Mukhopadhyay, J. Opt. **53**, 2278 (2024).

[31] S. Hazra, M. N. Sarfaraj, S. Mukhopadhyay, Brazilian Journal of Physics **54**, 64 (2024).

[32] A. H. Salari, S. Khosroabadi, M. Houshmand, Quantum Inf. Process **23**, 149 (2024).

[33] T. Poongodi, Intelligent Systems Reference Library **165**, 245 (2019).

*Corresponding author: gauravkumarbharti7@gmail.com